

# Real-Time C-Band Radar Observations of 1992 Eruption Clouds from Crater Peak, Mount Spurr Volcano, Alaska

By William I. Rose, Alexander B. Kostinski, and Lee Kelley

## CONTENTS

Abstract .....	19
Introduction .....	19
Acknowledgments .....	20
The 1992 Crater Peak eruptions .....	20
Description of the radar system .....	20
Use of radar for measurements of erupting column height .....	21
Size of ash particles detected by radar .....	23
Optimal use of radar systems during an eruption .....	25
Conclusions .....	25
References cited .....	26

## ABSTRACT

Repeated aircraft hazards in Alaska related to volcanic clouds have resulted in the use of a mobile C-band radar devoted to volcanic-cloud monitoring. The radar is located at Kenai, in range of several volcanoes in the Cook Inlet area. Three significant eruptions from the Crater Peak vent of Mount Spurr volcano (about 80 km from Kenai) in 1992 provided the first tests of the radar. The system constructs maps of the eruption columns and the drifting ash clouds for short periods (as long as 30 minutes) after eruption. The radar gives direct information about active eruptions in any weather conditions and allows estimates of the altitude of the column, which are useful for three-dimensional trajectory models of ash-cloud transport. It also allows an estimate of the eruption rate based on the ash-column height. However, such estimates may be lower than the true values because the very top of the eruption column, which may not contain coarse ash, may not be detected by the radar.

We conclude that the radar detects mainly ash particles, sized from about 1 millimeter to a few centimeters on the basis of three sources—the brief duration of the reflected radar signal, data from independent ground observations on the mass and size of particles which fell out of the reflected cloud, and the intensity of the reflected signal. The most intense reflections come from ash clouds with particles that range from 2 to 20 mm in diameter and with a total particle mass concentration of less than .01 to 1 g/m<sup>3</sup>.

The data are useful for constructing models of ash columns and deposition of coarse tephra. Radars are not useful for long-term volcanic cloud tracking because the large ash particles, that provide for strong radar signals fall out soon after an eruption. The radar does not detect smaller (<1–100 μm in diameter) ash particles in drifting volcanic clouds that can persist in the atmosphere for several days or more.

## INTRODUCTION

Since 1986, three volcanoes (Augustine, Redoubt, and Mount Spurr) have erupted in the Cook Inlet area of Alaska (fig. 1). Each of the eruptions has had a considerable impact on commercial aviation in south-central Alaska, particularly in Anchorage. Consequently, the National Weather Service (NWS) has significantly improved its capability of measuring and tracking ash clouds, in order to advise the aviation community about how to avoid ash clouds, which can be hazardous to jet aircraft. This report summarizes and interprets radar observations of ash clouds, made in real time during the 1992 Crater Peak eruptions, by a leased WR100-2 EEC meteorological C-band radar operated at Kenai, Alaska, opposite the volcanoes (fig. 1).

The radar was installed just prior to the 1992 activity. Three eruptions of the Crater Peak of Mount Spurr volcano in 1992 provided a first, robust test of the radar. The results provide data that are useful for real-time ash-cloud tracking and for forecasting cloud movement. Communication between the NWS office, the U.S. Geological Survey (USGS), and the Federal Aviation Administration (FAA) at Anchorage provides for the exchange of data and for timely and effective dissemination of eruption information to the public.

The data collected are also of volcanological interest. The usefulness of weather radar systems at active volcanoes was demonstrated at Mount St. Helens (Harris and others 1981; Harris and Rose, 1983). The heights of ash columns, which were measured during the eruptions, were used to calculate the eruption rate of ash. The radar system also mapped the extent of the most reflective parts of the ash cloud as it moved across Washington State.

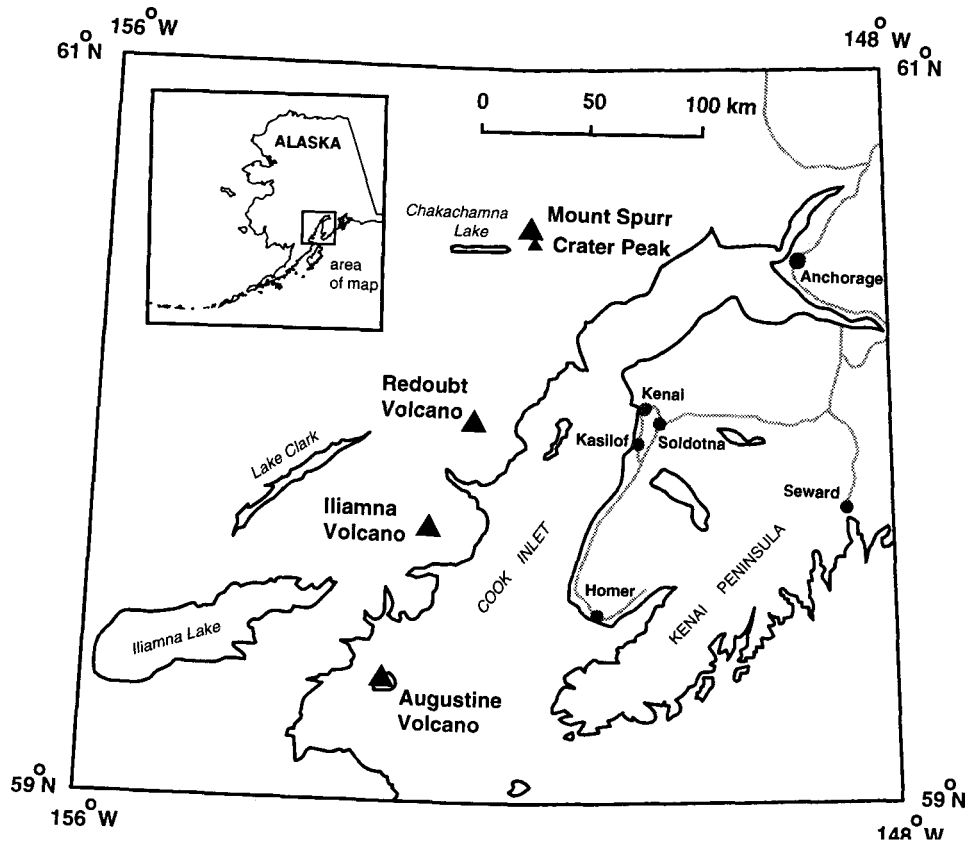


**Figure 1.** Index map of Cook Inlet area. The solid triangles represent volcanoes. Modified from Brantley (1990).

## ACKNOWLEDGMENTS

Funding for this project came from a grant from the Cooperative Program for Operational Meteorology Education and Training (COMET), a cooperative agreement between the National Weather Service and the University Corporation for Atmospheric Research, from NASA through grant NAG5-1838, and from NSF through grants ATM-9191075 and ATM 9116075. We thank people from the NWS staff in Anchorage, including Gary Hufford, Craig Bauer, Joel Curtis, and Ray Moore. Steve McNutt and Game McGimsey were helpful in providing data from the Alaska Volcano Observatory. Dave Harris, Steve McNutt, Jim Evans, Game McGimsey, Tina Neal, Rick Holasek, and Dennis Krohn provided helpful reviews.

## THE 1992 CRATER PEAK ERUPTIONS

A summary of data on the three Crater Peak eruptions of 1992 is given in table 1. The events were similar in many respects. They each lasted 3 to 4 hours and were marked by andesitic ash eruptions, which

produced roughly similar volumes of new ash (Neal and others, this volume). Each eruption resulted in narrow fallout blankets, which stretched for many kilometers from the volcano, and clouds that were much larger than those produced by the 1986 eruptions of Augustine Volcano (Holasek and Rose, 1991) and the 1989–90 eruptions at Redoubt Volcano (Schneider and Rose, 1994).

## DESCRIPTION OF THE RADAR SYSTEM

The Kenai radar is remotely operated by meteorologists stationed in the NWS forecast office in Anchorage, who communicate with the radar via modem. The main data displays are the range-height indicator (RHI), and the plan-position indicator (PPI). The RHI display is a vertical cross section of a reflecting cloud with a range and height scale (fig. 2). The PPI display is a horizontal cross section of the volcanic ash cloud on a scaled map background of Cook Inlet (fig. 2). The characteristics of the radar used are given in table 2. The radar's operation and performance were described in more detail by Serafin (1990).

**Table 1.** Data on 1992 Crater Peak eruptions, Mount Spurr volcano, Alaska.

[ADT, Alaska daylight time; AVO, Alaska Volcano Observatory; NWS, National Weather Service; \*, data unavailable; Sources of AVO data were Steve McNutt, Game McGimsey, Christina Neal, and Thomas Miller (oral commun., 1993). Anchorage International Airport closed at 6:10 p.m. ADT on 8/18/92]

	6/27/92	8/18/92	9/17/92
<b>AVO Observations</b>			
Eruption start, ADT -----	07:04 a.m.	4:42 p.m.	12:03 a.m.
Eruption end, ADT -----	11:07 a.m.	8:10 p.m.	3:39 a.m.
Volume of ash ( $\times 10^6 \text{ m}^3$ ) -----	12	14	15
<b>NWS Radar Observations</b>			
Eruption start ADT -----	*	*	12:10 a.m.
Eruption end ADT -----	*	6:13 p.m.	3:08 a.m.
Minimum volume of ash ( $\times 10^6 \text{ m}^3$ ) ----	*	a	16
Maximum column height, km -----	14.5	13.7	13.9
Time of maximum height, ADT -----	10:23 a.m.	4:55 p.m.	2:21 a.m.
<b>Anchorage International Airport Information</b>			
Service from airport -----	open	closed	open
Aircraft rerouted -----	yes	yes	yes

**Table 2.** Specifications of WR 100-22 EEC meteorological C-band radar used at Kenai, Alaska.

Parameter	Specification for the Kenai Radar
Primary power -----	115 volts, 60 cycle, single phase
Wavelength -----	5 cm
Peak power -----	250 KW
Pulse length -----	2 microseconds
Pulse repetition frequency -----	256 Hertz
Magnetron type -----	7156 A
Radio frequency -----	5500 to 5600 Megahertz
Antenna beam width -----	1.6 degrees
Receiver minimum detectable signal -----	-106 dBm (minimum)
Receiver IF -----	30 Megahertz
IF bandwidth -----	log 2 Megahertz
Receiver dynamic range -----	78 dB minimum

The reflectivity of the volcanic clouds is measured by comparing them to a standard equivalent reflectivity expressed in dBZ, which stands for decibels relative to a rain target with a reflectivity factor of  $1 \text{ mm}^6/\text{m}^3$ , for example,  $\text{dBZ} = 10 \log_{10} (Z/1 \text{ mm}^6/\text{m}^3)$ ; this allows inclusion of the natural range of meteorological precipitation clouds, within values of about 1 to more than 50 (Rinehart, 1991; Sauvageot, 1992). By choosing a range of dBZ values, contours of equal reflectivity are displayed on both the RHI and PPI images. Particle size and concentration may then be estimated from the measured reflectivities.

### USE OF RADAR FOR MEASUREMENTS OF ERUPTING COLUMN HEIGHT

When operated in the RHI (range-height indicator) mode and pointed directly toward the volcano (azi-

imuth of 328 in the case of Spurr), the radar can detect the top of the erupting column (fig. 3). Repeated measurements during the 3-hour eruption of September 16–17, 1992, give a record of the dynamics of the eruption of Crater Peak. The height measurements can be converted to eruption rates by the inversion of the Morton Equation (Morton and others, 1956; Wilson and others, 1978). Ignoring the effects of entrained atmospheric water vapor, we can then calculate the final height of a buoyant plume, given a constant eruption rate, to give an estimate of intensity of eruption with time (fig. 3). In simplified form, the Morton equation is  $H = 236.6 Q^{1/4}$ . H is the height of the erupting column in meters, and Q is the eruption rate in kilograms/sec. The constant, 236.6, includes an empirical constant in the correct dimensional form.

This measure of intensity compares well with the raw seismic signal measured during eruption, based

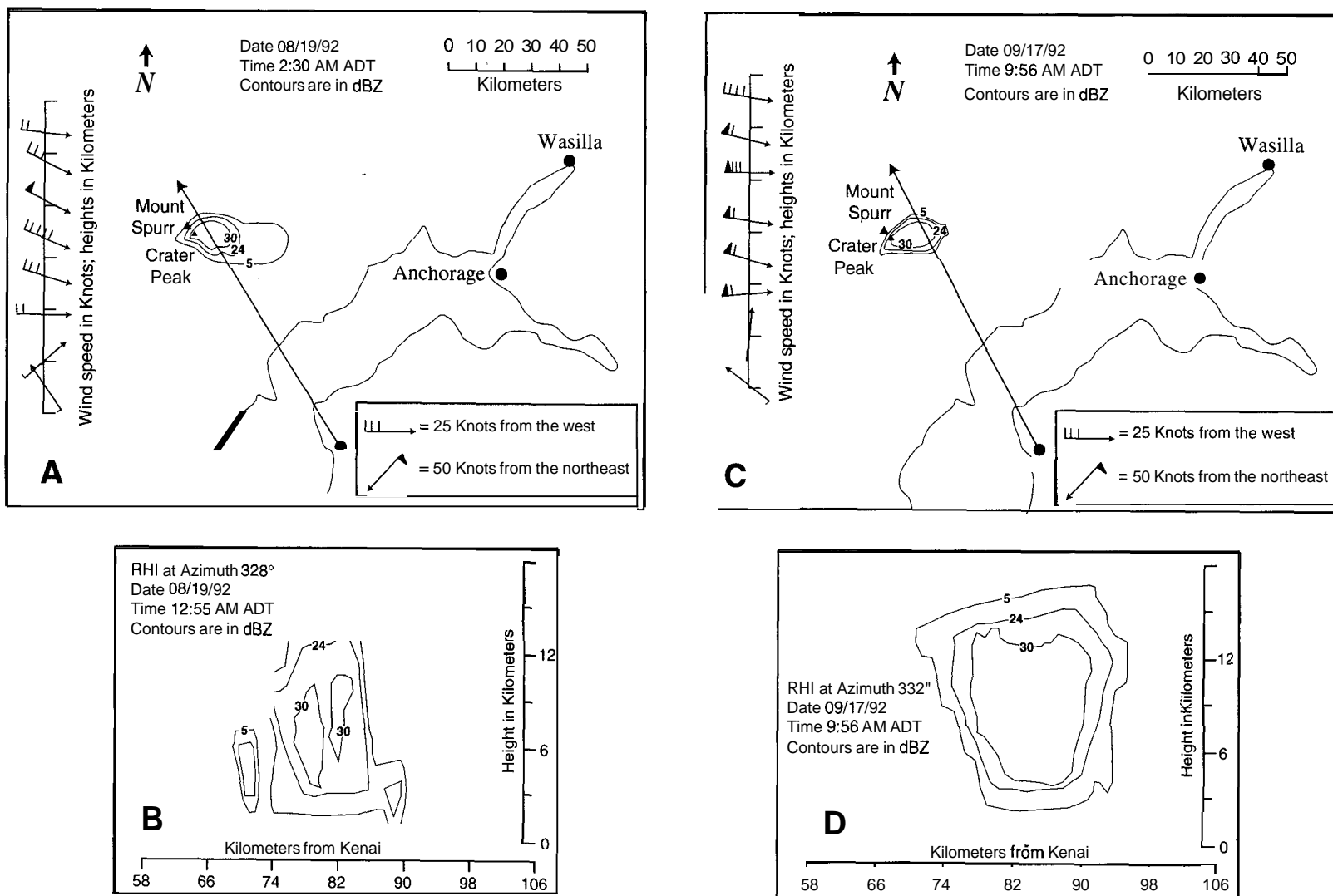
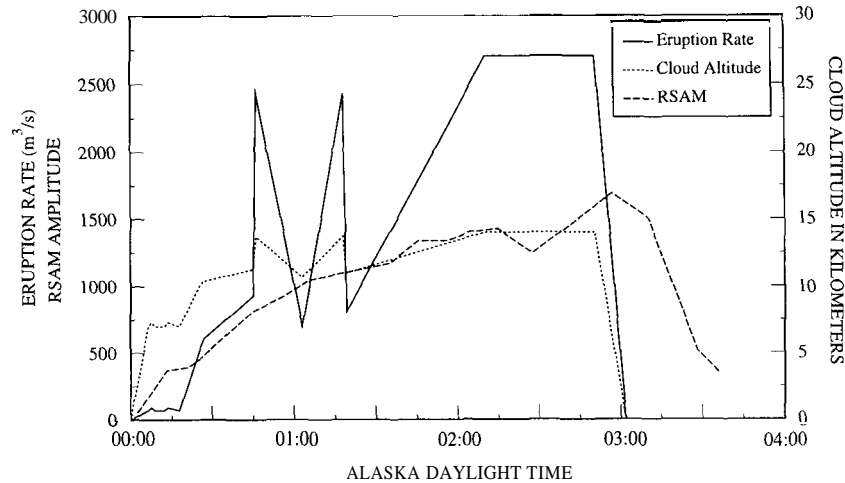


Figure 2. Data from C-band radar collected during the August (A and B) and September (C and D) Spurr eruptions. Times are listed in **GMT**. Both PPI and RHI formats are shown. The azimuth of the depicted RHI image is plotted on the PPI image. NWS upper-level wind data are plotted to the left of the PPI maps (altitudes shown in kilometers). The reflectivity of the volcanic clouds is measured by comparing them to a standard equivalent reflectivity expressed in **dBZ**, which stands for decibels relative to a rain target with a reflectivity factor of  $1 \text{ mm}^6/\text{m}^3$ .



**Figure 3.** Plots of eruption cloud maximum height versus time for the September 17, 1992, Spurr eruption as measured by C-band radar from Kenai. RHI recordings, with azimuths of 328°–332° (toward Crater Peak from Kenai), were used. A beam width correction was applied. Eruption rate versus time for the eruption is also plotted, derived from the radar height data and application of the Morton equation. RSAM seismic results from AVO (S. McNutt, oral commun., 1993), which are also measures of eruption intensity, are plotted for comparison. RSAM is a 1-minute average of seismic amplitudes from station BGL, 10 km from Crater Peak vent of Mount Spurr.

on real-time seismic amplitude measurement (RSAM) (Murray and Endo, 1992; fig. 3). The apparent eruption rate, estimated by the Morton equation and radar, can be integrated over the duration to get an estimate of the volume of ash emitted. The result is about  $16 \times 10^6 \text{ m}^3$ , which is almost the same as the amount estimated from ash fallout ( $15 \times 10^6 \text{ m}^3$ ). However, the radar could underestimate the column height because larger particles do not rise as high as smaller, less reflective ones (Carey and Sparks, 1986).

In summary, the radar offers a method of measuring the height of the eruption column, which is important for trajectory models of ash cloud movements. The systematic measurement of heights of the column is a way to monitor the eruption intensity and also gives a minimum estimate of mass of ash erupted.

### SIZE OF ASH PARTICLES DETECTED BY RADAR

The intensity of radar reflections is described by the Probert-Jones equation (Probert-Jones, 1962), which can be expressed in simplified form as  $P_r = R_c K^2 Z/R^2$ .  $P_r$  is the radar echo power received, and  $R_c$  is a radar constant containing the wavelength relations specific to the radar (peak power, antenna gain, beam width, and pulse length).  $R$  is the range of the

target.  $K^2$  is a refractive index factor, and  $Z$  is the target reflectivity factor, which is proportional to the product of the number density of reflecting particles and their radii, raised to the sixth power. Because the radar echoes are so strongly dependent on the size of the particles ( $r^6$  in the small dipole or Rayleigh approximation), the return signal detected by the radar is dominated by larger ash particles suspended in the cloud.

We observed that the radar system detected ash clouds only near the volcano and within about one half hour or less of actual eruption. The drifting cloud remains highly reflective to radar for a distance of only about 15 to 25 km from the volcano (fig. 2), which at the rate of winds measured, represents a transport time of about 15 to 30 minutes. We used data from figure 4 (Lapple, 1974) to estimate the size of ash particles that would fall to the ground in less than one half hour from heights of 14.2 km (47,000 feet) or less—time and height constrained by the Crater Peak radar observations. On the basis of these estimates, spherical particles with diameters of 1,000 microns (1 mm) or more would have terminal velocities (600 cm/sec) that would cause them to fall out within a half hour from 14.2 km. Because of the particles' extremely size-sensitive reflectivities and the rapid disappearance of the clouds from the radar, we think that the radar reflections we measured were caused by particles with diameters of 1,000 microns (1 mm) or larger.

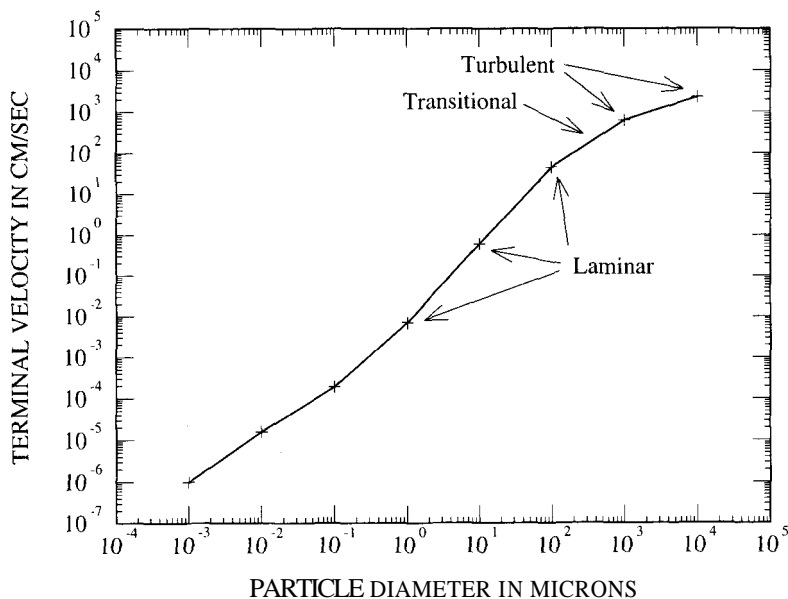


**Figure 4.** Terminal gravitational settling velocities of various size spheres with a density of  $2.0 \text{ g/cm}^3$  in dry atmosphere at  $25^\circ\text{C}$  and 1 atm (Laple, 1974).

A cross section of the cloud that was about 7 km downwind from the crater is shown in figure 3, and this cloud section shows very strong reflections (30 dBZ). A radar reflection is caused by the summation of all of the particles multiplied by their individual reflectivities. Consequently, a large number of small particles can have a reflectivity equal to a small number of large ones. Therefore, other data are necessary to determine the characteristics of the cloud.

In this case, we have excellent additional data: the time it takes for the radar image to disappear and the size and mass of the particles that fell out of the section imaged. These radar reflections cannot be produced from very large ash particles (greater than 3 cm), because their higher terminal velocities would cause them to fall out before drifting 7 km. On the basis of prevailing winds at appropriate altitudes (about 50–60 knots or 80–96 km/hr) at the time, we estimate that the cloud 7 km downwind is about 5 minutes old. Spheres with a density of  $2 \text{ g/cm}^3$ , which were larger than about 3 cm, would be completely removed from a 14-km-high cloud within 5 minutes. We should expect that ash particles, which are not spherical, will have greater atmospheric drag and, therefore, slower terminal velocities, but particles with diameters much larger than a few centimeters are not likely to be present in the cloud section shown in figure 2.

We compared the data on radar reflectivity of volcanic ash (Harris and Rose, 1983; Rose and Kostinski, 1994) to see what combinations of particle mass and size could explain the observed intensity of

radar reflection. The theoretical reflectivity results, calculated for identical, spherical particles with a volcanic ash refractive index factor ( $K^2$ ) of 0.3, which is about one-third that of liquid water (0.93), are shown in figure 5. The maximum reflection, seen in the drifting cloud 7 km downwind (30 dBZ), corresponds to more than  $100 \text{ g/m}^3$  of ash particles with a radius of 0.25 mm,  $20 \text{ g/m}^3$  of ash particles with a radius of 0.5 mm,  $0.7 \text{ g/m}^3$  of ash with a radius of 1 mm, or less than  $0.01 \text{ g/m}^3$  with a radius of 4 mm. Because the radar reflection shown in figure 2 is thousands of meters high, a particle-mass concentration of  $20 \text{ g/m}^3$  implies a fallout thickness of much more than 1.5 m. Consequently, the mass concentrations of  $20 \text{ g/m}^3$  or higher are impossible because the observed fallout data are inconsistent with them.

The isopach maps of fallout on September 17, 1992, show that the thickness 7 km down the dispersal axis is about 10 cm, and the grain size is mainly between 1 and 30 mm (R.G. McGimsey, oral commun., 1993). This data, along with our observation that the radar signal disappeared after 30 minutes, implies that most of the particles which reflected the radar signal were 2 to 20 mm in diameter and the particle concentrations of the reflecting cloud ranged from less than  $0.01$  to about  $1 \text{ g/m}^3$  (shown by the shaded area of fig. 5). In comparison, Harris and Rose (1983) estimated that the particle-mass concentrations for the Mount St. Helens eruption clouds of May 18, 1980, and March 19, 1982, were  $3 \text{ g/m}^3$  and  $0.2 \text{ g/m}^3$  respectively, similar to the Crater Peak estimates.

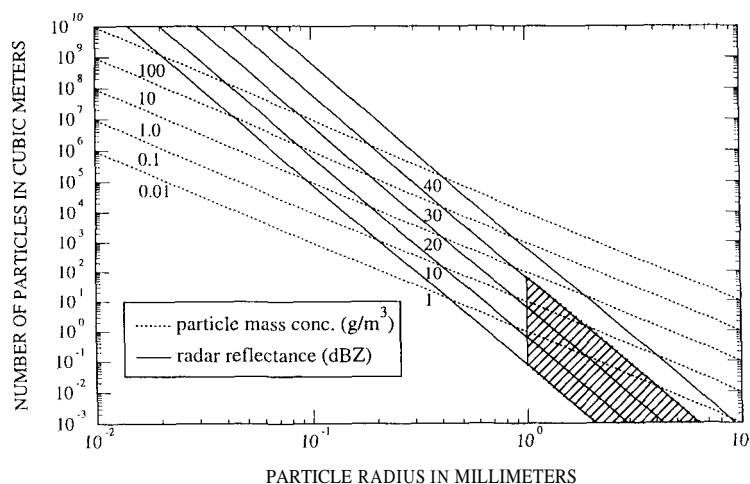


Figure 5. Relation between radar reflection returned (measured in decibels relative to a rain target or dBZ), the total mass of ash particles per unit volume (measured in grams per cubic meter), the number of particles per cubic meter, and the radius of the particles in mm. This figure is based on idealized assumptions: single size for particles, perfect spherical shape of all particles, and a refractive index factor which is about one-third of that for water droplets. Cross-hatched portion probably most closely approximates conditions in the 1992 eruption clouds from Crater Peak of Mount Spurr, which were detected by the C-band radar. This approximation is based on the duration of radar reflection and observed size of fallout.

## OPTIMAL USE OF RADAR SYSTEMS DURING AN ERUPTION

Aircraft traveling at high speeds must get timely warning of ash clouds. During eruptions, radar measurements of ash can be directly communicated from the NWS to the Anchorage Air Route Traffic Control Center (ARTCC) so that aircraft in immediate danger can be diverted and decisions on possible airspace closures can be made.

Because the returns of the radar signal come mainly from large (1–30 mm) ash particles, the radar measurements can only be made during and immediately following actual eruptions. At the beginning of the eruption, the radar in the RHI mode makes initial detection and height measurements.

During the September 16–17, 1992, eruption of Crater Peak vent, the radar was able to verify the Alaska Volcano Observatory's (AVO) seismic indications of activity at Crater Peak within a few minutes. The eruption began at 10:36 a.m. ADT on September 16, and the initial activity lasted 16 minutes. At 12:03 a.m. ADT on September 17, AVO called NWS alerting them that an eruption was likely in progress. At 12:10 a.m. ADT, the Kenai radar verified a volcanic ash cloud above Mount Spurr. Later that morning, at just after 3:00 a.m. ADT, AVO called NWS with a notification

that the eruption had ended. During the call from AVO, the volcano was scanned, and the ash cloud observed by the radar was detached from the volcano. Within 20 minutes, the radar could detect no ash cloud.

Radar detection is valuable in many ways. Radar-based detection is especially important during conditions of poor visibility, when other types of observations are difficult. Radar height measurements of the ash cloud are inputs to the production of a three-dimensional ash dispersion tracking model, which the NWS is implementing to forecast volcanic cloud positions. In cooperation with AVO, the NWS works with the Alaska Division of Emergency Services to identify those areas of the state that will most likely be affected by ash fallout.

A new generation WSR-88D radar system was installed in 1994 at Kenai, Alaska. The WSR-88D is a modern S band ( $\lambda = 10\text{--}11\text{ cm}$ ), doppler radar, which could provide some advantages for volcanic cloud mapping, including information on radial velocities in and around the ash cloud.

## CONCLUSIONS

The 5-cm radar operated from Kenai was successfully used to map ash clouds from Crater Peak about 80 km away. The radar signal is dominated by

ash particles larger than about 1,000 microns in diameter. We were able to use ground measurements of the sizes and masses of fallout particles that fell from the ash cloud as well as the dynamics of fallout constrained by the duration of the radar reflection to tell us that the largest radar reflections were mainly caused by ash particles that were between 2 and 20 mm in diameter.

Radar can also be used to measure the height of the ash cloud, but it may underestimate the height because it does not respond to smaller ash particles, which rise higher. C-band radar does not detect distal parts of the ash cloud, which have an atmospheric residence time longer than 30 minutes, because the larger more reflective ash particles drop out.

The Kenai radar is the first type of remote sensor to actually view ash clouds. Its all weather capability fills the data gaps of satellite data as well as other observational methods and the real-time use of a radar provides an excellent way to corroborate the seismic indications of actual eruptions. Radar provides vital, immediate warning and information to the aviation community.

The radar system offers, for the first time, the opportunity of mapping internal structure of dense proximal ash plumes during eruptions. This capability can supply data to volcanologists who are interested in modeling eruption columns (Wilson and others 1978; Carey and Sparks, 1986; Bursik and others, 1992). Because of the radar's sensitivity to larger particles, such a system would be particularly valuable in testing models for the fallout of larger particles, such as the one developed by Bursik and others (1992).

## REFERENCES CITED

- Brantley, S.R., 1990, The eruption of Redoubt Volcano, Alaska, December 14, 1989–August 31: U.S. Geological Survey Circular 1061, 33 p.
- Bursik, M.I., Sparks, R.S.J., Gilbert, J.S., and Carey, S.N., 1992, Sedimentation of tephra by volcanic plumes: I. Theory and its comparison with a study of the Fogo A plinian deposit, Sao Miguel (Azores): *Bulletin of Volcanology* v. 54, p. 329–344.
- Carey, S.N., and Sparks, R.S.J., 1986, Quantitative models of the fallout and dispersal of tephra from volcanic eruption columns: *Bulletin of Volcanology*, v. 48, p. 109–125.
- Harris, D.M., Rose, W.I., Roe, R., and Thompson, M.R., 1981, Radar observations of ash eruptions, *in* Lipman, P.W., and Mullineaux, D.R., eds., *The 1980 Eruptions of Mount St. Helens*, Washington: U.S. Geological Survey, Professional Paper 1250, p. 323–333.
- Harris, D.M., and Rose, W.I., 1983, Estimating particle sizes, concentrations, and total mass of ash in volcanic clouds using weather radar: *Journal of Geophysical Research*, v. 88, p. 10968–10983.
- Holasek, R.E., and Rose, W.I., 1991, Anatomy of 1986 Augustine eruption clouds as recorded by multi-spectral image processing of digital AVHRR weather satellite data: *Bulletin of Volcanology*, v. 53, p. 420–435.
- Lapple, C.E., 1974, Characteristics of Particles and Particle Dispersoids, *in* Perkins, H.C., *Air Pollution*, New York, McGraw-Hill, p. 224–225.
- Morton, B.R., Taylor, G., and Turner, J.S., 1956, Turbulent gravitational convection from maintained and instantaneous sources: *Proceedings of Royal Society (London) Ser A*, v. 234, p. 1–23.
- Murray, T.L., and Endo, E.T., 1992, A real-time seismic amplitude measurement system (RSAM): *United States Geological Survey Bulletin* 1966, p. 5–10.
- Probert-Jones, J.R., 1962, The radar equation in meteorology: *Quarterly Journal, Royal Meteorological Society*, v. 88, p. 485–495.
- Rinehart, R.E., 1991, *Radar for Meteorologists*, University of North Dakota, Grand Forks.
- Rose, W.I., and Kostinski, A.B., 1994, Radar remote sensing of volcanic clouds, *in* Casadevall, T., ed., *Proceedings of the First International Symposium on Volcanic Ash and Safety*: U.S. Geological Survey Bulletin 2047, p. 391–396.
- Sauvageot, H., 1992, *Radar Meteorology*, Artech House.
- Schneider, D., and Rose, W.I., 1994, Observations of the 1989–90 Redoubt Volcano eruption clouds using AVHRR satellite imagery, *in* Casadevall, T., ed., *Proceedings of the First International Symposium on Volcanic Ash and Aviation Safety*: U.S. Geological Survey Bulletin 2047, p. 405–418.
- Serafin, R.J., 1990, *Meteorological Radar*, *in* Skolnik, M., *Radar Handbook*, 2d ed.: New York, McGraw-Hill, p. 23.1–23.33.
- Wilson, L., Sparks, R.S.J., Huang, T.C., and Watkins, N.D., 1978, The control of volcanic column heights by eruption energetics and dynamics: *Journal of Geophysical Research*, v. 83, p. 1829–1836.